



UNIVERSITÀ POLITECNICA DELLE MARCHE
Repository ISTITUZIONALE

A comparative study on the possible cytotoxic effects of different nanostructured lipid carrier (NLC) compositions in human dermal fibroblasts

This is a pre print version of the following article:

Original

A comparative study on the possible cytotoxic effects of different nanostructured lipid carrier (NLC) compositions in human dermal fibroblasts / Bruge', Francesca; Damiani, Elisabetta; Marcheggiani, Fabio; Alessia, Offerta; Carmelo, Puglia; Tiano, Luca. - In: INTERNATIONAL JOURNAL OF PHARMACEUTICS. - ISSN 0378-5173. - ELETTRONICO. - 495:(2015), pp. 879-885. [doi.org/10.1016/j.ijpharm.2015.09.033]

Availability:

This version is available at: 11566/227847 since: 2022-06-01T14:28:44Z

Publisher:

Published

DOI:doi.org/10.1016/j.ijpharm.2015.09.033

Terms of use:

The terms and conditions for the reuse of this version of the manuscript are specified in the publishing policy. The use of copyrighted works requires the consent of the rights' holder (author or publisher). Works made available under a Creative Commons license or a Publisher's custom-made license can be used according to the terms and conditions contained therein. See editor's website for further information and terms and conditions.

This item was downloaded from IRIS Università Politecnica delle Marche (<https://iris.univpm.it>). When citing, please refer to the published version.

(Article begins on next page)

**A COMPARATIVE STUDY ON THE POSSIBLE CYTOTOXIC EFFECTS OF
DIFFERENT NANOSTRUCTURED LIPID CARRIER (NLC) COMPOSITIONS
IN HUMAN DERMAL FIBROBLASTS**

Francesca Bruggè^{a†}, Elisabetta Damiani^{b†*}, Fabio Marcheggiani^a, Alessia Offerta^c,
Carmelo Puglia^c, Luca Tiano^a

^aDipartimento di Scienze Cliniche Specialistiche ed Odontostomatologiche, ^bDipartimento di
Scienze della Vita e dell'Ambiente, Università Politecnica delle Marche, Via Brecce Bianche,
60131 - Ancona, Italy

^cDipartimento di Scienza del Farmaco, Università degli Studi di Catania, Viale Andrea Doria 6,
95125 - Catania, Italy

[†] Equal contribution

*Corresponding author:

Dr. Elisabetta Damiani

Dipartimento di Scienze della Vita e dell'Ambiente

Università Politecnica delle Marche

Via Brecce Bianche

60131 - Ancona, ITALY

Email: e.damiani@univpm.it

Phone: +390712204135

Fax: +390712204398

ABSTRACT

Nanostructured lipid carriers (NLC) are widely used for topical delivery of active ingredients into the skin for both local and systemic treatment. But concerns have been raised regarding their potential nanotoxicity. To understand the role of NLC composition in terms of cytotoxicity and pro-oxidant effects, we investigated cell viability and intracellular levels of ROS (reactive oxygen species) production in human dermal fibroblasts (HDF) incubated with five NLC formulations differing in their solid lipid composition. HDF and NLC were also exposed to UVA irradiation in order to evaluate the behavior of NLC under realistic environmental conditions which might promote their instability. Using the Guava via-count assay, all nanoparticles, except for those formulated with Compritol 888 ATO, showed a significant decrease in live cells and a parallel increase in apoptotic or dead cells compared to the control, either before and/or after UVA irradiation (18 J/cm²). NLC formulated with Geleol™ Mono Diglycerides resulted the most cytotoxic. A similar trend was also observed when intracellular ROS levels were measured in HDF incubated with NLC: there was increased ROS content compared to the control, further exacerbated following UVA. NLC formulated with Dynasan 118 were particularly susceptible to UVA exposure. The results indicate which could be the most suitable candidates for formulating NLC that are biocompatible and non-cytotoxic even when exposed to UVA and hence help direct future choices during the formulation strategies of these delivery systems. Of those tested, Compritol 888 ATO appears to be the best choice.

Keywords: Nanostructured lipid carriers (NLC); lipid composition; cytotoxicity; reactive oxygen species; UVA

1. INTRODUCTION

Lipid nanoparticles are becoming an emerging tool for lipid-based substances delivery across epithelial barriers. Nanocarriers enhance drug permeation and expand the range of molecules that can be delivered by the transdermal route. Basically, they are colloidal particles composed of a biocompatible/biodegradable lipid matrix which is solid at body temperature and exhibits a size <200 nm. These particles have the advantage of increasing drug solubility by enhancing the dissolution kinetic profile and improving the bioavailability of the active substance (Gokce et al., 2012). They have all the advantages of other colloidal drug carrier systems like liposomes, polymeric nanoparticles, and emulsions, but at the same time the drawbacks associated with them are avoided or minimized (Joshi and Muller, 2009). For this reason, they can be regarded as a natural and logical evolution of the above mentioned nanocarriers. In fact, the first generation of lipid nanoparticles (SLN) derives from the substitution of a nanoemulsion oil phase (liquid) with a solid lipid. The main advantages associated with SLN compared with other colloidal systems are high biocompatibility, good physical stability, possibility of controlled release of drug and active substances, easy large scale production and cheap raw materials. Despite these important features, they possess some limitations such as drug expulsion phenomena, particle concentration in the aqueous dispersion ranging from about 1% to a maximum of only 30% and insufficient total drug payload due to the limited solubility of drugs in the solid lipid (Kupetz and Bunjes, 2014; Mehnert and Mader, 2001). To overcome the limitations of SLN, NLC (nanostructured lipid carriers) were developed representing the second generation of lipid nanoparticles. This was achieved by the addition of a liquid lipid to form a blend of solid and liquid lipids. This addition distorts the formation of perfect lipid crystals minimizing drug expulsion phenomena and increasing drug loading compared with SLN (Muller et al., 2002; Pardeike et al., 2010; Teeranachaideekul et al., 2007; Yue et al., 2010). This new approach has also lead to significant improvements in promoting the bioavailability through oral, intravenous and intraperitoneal routes of administration and permeability through biological barriers such as the hematoencephalic one and skin (Muller and Keck, 2004; Puglia and Bonina, 2012; Puglia et al., 2012).

In this regard, the delivery of active substances to the skin presents several challenges, since this tissue compared to other epithelial tissues is not optimized to favor the absorbance of substances from the external environment, but rather, to provide a protective barrier. It is composed of two main structural compartments: the epidermis, an effective self-renewing barrier on the surface, largely composed of hyperkeratinized cells, and a deeper layer of metabolically active cells and extracellular matrix defined as dermis. The major cellular component of the dermis are dermal fibroblasts (HDF) that are responsible for the synthesis of molecules involved in mechanical function, hydration, and elasticity (collagen, elastin, hyaluronic acid, etc.). The delivery of active components that should address specific physio-pathological conditions, such as compounds endowed with anti-inflammatory and anti-ageing properties, should be able to efficiently reach this compartment, and nanolipid carriers could represent an effective strategy to maximize delivery.

In fact, nanolipid carriers have been shown to provide controlled release profiles through different epithelia (Jenning and Gohla, 2001; Muller et al., 2006). The small size ensures close contact with the

stratum corneum and can increase the amount of drug absorbed by the skin. Lipid nanoparticles are also able to enhance the chemical stability of compounds sensitive to light, oxidation, and hydrolysis (Gokce, Korkmaz et al., 2012). Moreover, they may be composed of physiological and biodegradable lipids which are generally recognized as safe (GRAS) (Mehnert and Mader, 2001; Muller et al., 2000) thus improving biocompatibility. In fact, the irritant potential for skin and eyes as well as cytotoxicity for normal human keratinocytes is low (Kuchler et al., 2010).

Nonetheless, concerns have risen over the use of nanomaterials in biology, and different studies have pointed to the limitations over their use in biological systems both *per se* and synergistically, exacerbating the noxious effect of environmental insults (i.e. UV radiation, xenobiotic-induced oxidative damage). For instance, nanosized lipid particles have been shown to intensify the phototoxicity of UV radiation in HDF (Bruge et al., 2013) while nanosized titanium dioxide and polystyrene particles have been reported to induce oxidative stress in human and murine cell lines (Jaeger et al., 2012; Xia et al., 2006). Nanoparticles have also been shown to interact with cellular sensitive sites promoting reactive oxygen species (ROS) production at the mitochondrial level, interfering both with the mitochondrial respiratory chain and cytochrome P450 function (Huerta-Garcia et al., 2014; Kulthong et al., 2012; Periasamy et al., 2014). Concerning with NLC, we recently observed a potential pro-oxidant effect of NLC in non-irradiated and UVA-exposed HDF that might affect cell function and viability, therefore limiting their possible application in biological systems (Bruge, Damiani et al., 2013).

One of the most important factors for potential nanotoxicity is the lack of biodegradability of nanomaterials which can be taken up and retained in the reticuloendothelial system, hence preliminary investigations on the toxicity of nanomaterials routinely begin with cytotoxicity assays. In an attempt to understand the role of the composition of NLC in terms of cytotoxicity and pro-oxidant effects, in the present study we investigated cell viability and intracellular ROS levels production in HDF incubated with five different blank NLC formulations differing in their lipid composition. The experiments were also carried out under UVA irradiation in order to evaluate the behavior of the tested nanoparticles under feasible environmental conditions which might promote instability of the tested NLC.

130

2. MATERIALS AND METHODS

2.1 Materials

Precirol™ ATO 5 (Glycerylpalmito-stearate), Compritol™ 888 ATO (Glyceryldibehenate) and Geleol™ Mono and Diglycerides (Glycerylmonostearate) were a gift from Gattefossè (Milan, Italy), Dynasan™ 118 (Tristerin) was provided by Cremer Oleo GmbH & Co. (Hamburg, Germany), Softisan™ 100 (Hydrogenated Coco-Glycerides) was obtained by Sasol Germany (Hamburg, Germany). Miglyol™ 812 (caprylic/capric triglycerides) was provided by Eingemann & Veronelli S.p.A (Milan, Italy). Lutrol™ F68 (Poloxamer 188) was a gift from BASF ChemTrade GmbH (Burgbernheim, Germany). When not specified, all other chemicals and reagents were of the highest purity grade commercially available.

140

2.2. NLC preparation

Batches of NLC suspensions containing different ingredients (Table 1), were prepared by ultrasonication method following the procedure reported elsewhere (Puglia and Bonina, 2012). Briefly, the solid lipid (10.5 g) was melted at a temperature ten degrees higher than its melting point and Miglyol™ 812 (4.5 g) was added. The melted lipid phase was dispersed in a hot surfactant solution composed of Lutrol™ F68 (0.5 g) using a high-speed stirrer (UltraTurraxT25, IKA-WerkeGmbH & Co. KG, Staufen, Germany) at 8000 rpm. Formulations A-E were characterized by different solid lipids and therefore the temperature of the hot surfactant solution corresponded to that of the oily phase reference. The obtained pre-emulsion was ultrasonified using a UP 400 S (Ultra-schallprozessor, Dr. Hielscher GmbH, Germany) for 2 min. Then the hot dispersion was cooled in an ice bath and dispersed in cold water under high-speed homogenization (UltraTurrax T25; IKA-Werke GmbH & Co. KG, Staufen, Germany) at 8000 rpm for 5 min in order to solidify the lipid matrix and to form NLC suspensions.

2.3. Particle size distribution and zeta potential measurements

Mean particle size of the lipid dispersions was measured by photon correlation spectroscopy (PCS). A Zetamaster (Malvern Instrument Ltd., Sparing Lane South, Worcs, England), equipped with a solid-state laser having a nominal power of 4.5 mW with a maximum output of 5 mW at 670 nm, was employed. Analyses were performed using a 90° scattering angle at 20 ± 0.2 °C. Samples were prepared by diluting 10 µL of A-E suspensions with 2 mL of deionized water previously filtered through a 0.2 µm Acrodisc LC 13 PVDF filter (Pall-Gelman Laboratory, Ann Harbor, Michigan). During the experiment, the refractive index of the samples always matched the liquid (toluene) to avoid stray light. The Zeta (ξ) potential was automatically calculated from the electrophoretic mobility based on Smoluchowski's equation (Eq. 1):

Eq. 1
$$v = \left(\frac{\varepsilon \cdot E}{\eta} \right) \xi$$

where v is the measured electrophoretic velocity, η is the viscosity, ε is the electrical permittivity of the electrolytic solution, and E is the electric field. The accuracy was 0.12 µm cm/V s for the aqueous systems. The samples were suspended in distilled water and the measurements were recorded at 25 °C.

2.4 Cell cultures

HDF were cultured in 25 cm² flasks in MEM supplemented with 10% fetal bovine serum (GENENCO, South America Origin), penicillin (100 U/mL), streptomycin (100 g/mL) and L-glutamine (2 mM), at 37 °C in a CO₂ Heraeus BB15 incubator (ThermoScientific) under humidified atmosphere. For cell culture maintenance, the medium was changed every 2-3 days and cells were passaged at 80% confluence by trypsinization. For the experiments, cells were seeded in 24 well plates at an optimal density of 14×10^3 cells/cm².

2.5 NLC supplementation

Cells at 75% confluence were incubated in the presence of five different NLC formulations at a final concentration of 0.26 mg/mL in culture medium in analogy with our previous data (Bruge, Damiani et al., 2013). Control cells were incubated with medium alone (CTRL). After 24 h of incubation at 37°C, 5% CO₂,
180 the cells were either tested immediately or subjected to UVA exposure prior to further determinations.

2.6 UVA exposure

For UVA irradiation, cells were washed with PBS and covered with a thin layer of PBS prior to exposure. The culture plate lids were removed and replaced with a 2 mm thick sterilized quartz slab. The cell culture
185 plates were placed on a brass block embedded on ice in order to reduce any evaporation at a distance of 20 cm from the above incoming light source. For flow cytometric determinations, cells were irradiated for 10 min (18 J/cm²). UVA irradiation time was chosen following a time course experiment in the range of 10-60 min and the selected dose was the lowest one showing a significant effect compared to the non-irradiated control sample. As UVA irradiating source, a Philips Original Home Solarium sun lamp (model HB406/A;
190 Philips, Groningen, Holland) equipped with a 400 W ozone-free Philips HPA lamp, UV type 3, delivering a flux of 23 mW/cm² between 300 and 400 nm, was employed. The dose of UVA was measured with a UV Power Pack Radiometer (EIT Inc., Sterling, USA), while the emission spectrum was checked using a Stellar-Net portable spectroradiometer (Tampa, FL, USA) and is reported elsewhere (Venditti et al., 2008).

195 2.7 Cell viability and intracellular ROS assays

For determination of cell viability, the Guava Via-count solution (Merck, Millipore) which is a fluorescent stain formulation that provides accurate detection of viable, apoptotic and dead cells in flow cytometry was used. As indicator of intracellular ROS formation, the leucodye, carboxy-2,7-dichlorofluorescein diacetate (carboxy-H₂DCFDA) (Invitrogen) was employed. This is a lipophilic probe
200 which is actively incorporated into live cells where it is retained by the activity of esterases that expose negatively charged residues upon cleavage of acetates. Following oxidation by intracellular ROS, it then becomes fluorescent (Hafer et al., 2008). To the non-irradiated and UVA-irradiated samples, PBS was removed and a solution of carboxy-H₂DCFDA 10 µM in PBS was added to each sample, and incubated in the dark for 30 min at 37°C. After trypsinization, cells were harvested and centrifuged at 600g for 5 min and
205 the cell pellet was resuspended in approximately 50 µl of culture medium. An aliquot of 20 µL from each sample was then added to 180 µL of a solution of Guava Via-count. The analyses for cell viability and intracellular ROS production were then conducted simultaneously on a Guava Easycyte flow cytometer (Millipore) using an excitation wavelength of 488 nm. Emissions were recorded using the green channel for carboxy-DCF and the red and yellow channels for the Via-count dye, using the following gain settings: FSC
210 29.3; SSC 23.6; G18.2; Y49.4; R22.6 and a threshold of 1000 on FSC. Fluorescence intensity was recorded on an average of 5,000 cells from each sample. Experiments were carried out at least in triplicate and results were analyzed using In-cytes software.

The cell viability analysis is based on the population distribution which allows to discriminate the percentage of cell debris (R-/Y-), live cells (R+/Y-) and dead cells (R+/Y+). Moderately yellow, positive
215 cells may be considered as a marker of apoptosis, similarly to supravital propidium iodide staining. This assumption has been validated in specific cell lines with Annexin staining by Millipore.

For analysis of intracellular ROS formation, three regions relative to low, mid and high levels of fluorescence were defined, based on preliminary experiments on cells exposed to UVA. UVA exposure leads to a remarkable increase in intracellular ROS formation that can be easily monitored by observing a
220 large shift in green fluorescence (FL1) due to the oxidized form of carboxy-H₂DCFDA (carboxy-DCF): this shift is proportional to ROS formation and is considered as the positive control. As negative control, the fluorescence distribution of non-irradiated cells was used. Based on the fluorescence distribution between non-irradiated and irradiated cells, three gates were arbitrarily set to define the three regions. Namely, low ROS (region representing 50% of population of non-irradiated cells); high ROS (region representing 50% of
225 population of irradiated cells); mid ROS (region lying in between these two populations). These settings were then maintained for all subsequent experiments for irradiated and non-irradiated cells in the presence of NLC, and the relative percentage of cells in each region was calculated. Counterstaining with Via-count was necessary in order to evaluate intracellular levels of ROS *only* in viable cells. In fact, exclusion of cells with compromised cell membrane integrity is essential in order to avoid false negatives due to loss of carboxy-
230 H₂DCFDA from permeable cells.

2.8 Statistical analysis

Mean value and standard deviation (S.D.) were calculated. All data were analyzed using one-way Anova with post-hoc analysis using Tukey's Honestly Significant Difference (HSD) method, assuming a
235 significance level of 5%. A value of $p < 0.05$ was considered statistically significant.

3. RESULTS

3.1. NLC preparation and characterization

A-E NLC suspensions were formulated using different excipients as reported in Table 1. The solid lipids
240 were chosen among the most popular excipients used to produce lipid nanoparticles. The strategy of formulation is represented by the ultrasonication method (US), a "cheap and fast" strategy, widely used to formulate homogeneous and nanosized particles (Puglia and Bonina, 2012). PCS analyses showed that all the NLC formulations were in the nanometric range and characterized by good homogeneity (Table 2). Moreover, formulation E showed a different trend with increased dimensions and a poor homogeneity (PDI
245 > 0.3). Zeta potential (ZP) is an important parameter that allows to predict NLC's physical stability and in theory, higher ZP values, either positive or negative, tend to stabilize particle suspension. Usually, particle aggregation is less likely to occur for charged particles with pronounced ZP ($> |20|$), due to the electrostatic repulsion between particles with the same electrical charge (Gonzalez-Mira et al., 2010). Concerning with

the A-E formulations, the analyses registered zeta potential values below -30 mV predicting good long-term stability for all the tested formulations.

3.2 Cell viability and intracellular ROS

The biocompatibility/cytotoxicity of the tested NLC was evaluated in UVA exposed and non-exposed HDF using the Guava Via-count assay. This test uses a mixture of two DNA binding dyes: a membrane permeant one stains all nucleated cells leaving cellular debris unstained in order to identify whole cells, and a membrane-impermeant dye that stains only damaged cells, enabling identification of apoptotic and dead ones.

As shown in Fig. 1A, all tested nanoparticles exhibited very mild cytotoxicity with viability values ranging between 80%-90% compared to the control sample. However, within the limits of biocompatibility, all tested nanoparticles, except for NLC-C and NLC-A, showed a significant decrease in live cells ($p<0.05$) and a parallel increase in apoptotic cells compared to the control. The most cytotoxic appears to be NLC-B since an almost 10-fold significant increase in dead cells was observed associated with a concomitant, significant decrease in live cells and apoptosis induction. Following 10 min of UVA exposure, a remarkable cytotoxic effect was detected as can clearly be seen in Fig. 1B which shows more apoptotic and dead cells compared to the live ones. In fact, NLC-free control cells showed a very different distribution in live, apoptotic and dead cells compared to unexposed cells (Fig. 1A). In relation to NLC exposure to UVA, the presence of all tested formulations with the exception of NLC-C and NLC-E, enhanced the UV-induced cytotoxicity in terms of percentage of dead cells. In particular, the percentage of dead cells was significant for NLC-B (+468%), NLC-A (+175%) and NLC-D (+116%). Taken together, these data highlight a mild, cytotoxic effect for some of these formulations, especially in the case of NLC-B. The exception is NLC-C which showed no significant cytotoxicity both before and after UVA irradiation.

Fig. 2A shows intracellular ROS levels measured in viable cells only, for all non-irradiated samples incubated with NLC compared to the NLC-free control. Incubation with NLC significantly decreased the percentage of cells containing low levels of ROS and increased the percentage of cells with mid levels of ROS for all tested formulations with the exception of NLC-A. However, after UVA exposure (Fig. 2B) this latter formulation showed significantly increased levels of high ROS with a concomitant decrease in the levels of mid ROS. NLC-E also showed a significant increase in the levels of high ROS following UVA irradiation. The ROS distribution measured with the other formulations resulted not significantly different from the UVA irradiated control. Worthy of note, is the fact that UVA irradiation remarkably affects the distribution of cells in relation to their intracellular ROS content (Fig. 2B) compared to the non-irradiated samples (Fig. 2A): UVA exposure leads to a marked decrease in the content of low and mid ROS with a concomitant rise in the content of high ROS.

4. DISCUSSION

The present study focused on the role of the lipid-core material in modulating the cytotoxicity of nanolipid carriers. Biocompatibility of nanolipid carriers is an emerging issue in the use of solid-liquid nanocarriers. In fact, these molecules have shown a remarkable ability to penetrate cellular membranes with promising applications in gene and pharma delivery. On the other hand, a growing number of bioavailability studies have consistently shown a non-negligible level of cytotoxicity exerted by unloaded control nanoparticles. These indications are thoroughly reviewed in a recent article by Doktorovova et al. that summarizes data available from cytotoxicity and oxidative stress in the available literature up to December 2013 (Doktorovova et al., 2014).

In a recent study (Bruge, Damiani et al., 2013), we documented a mild cytotoxicity of NLC that was aimed at evaluating the effects of reduced and oxidized Coenzyme Q₁₀ (CoQ₁₀) loaded in NLC on HDF exposed to UVA radiation. We showed that NLC nanoparticles are not neutral carriers since they are able to induce mild oxidative stress and oxidative damage in HDF at concentrations used for topical applications. Moreover, their use under environmental stimuli, such as UVA radiation present in sunlight, enhanced UV-dependent oxidative stress/damage. NLC loading with CoQ₁₀, a potent lipophilic antioxidant, was only able to mitigate the synergistic toxic effect but was not able to provide enhanced cellular antioxidant defence.

As pointed out in (Doktorovova, Souto et al., 2014), cytotoxicity of NLC might be influenced both by the nature of the lipid-core material used as well as by the surfactant, however the specific contribution of these components is difficult to extrapolate from the literature due to the lack of reports dealing with the comparison of NLC formulations. In the present investigation we directly compared five NLC formulations containing the same surfactant (Lutrol 0.05%) but different solid lipid components. The lipids used to prepare NLC are usually triglycerides, fatty acids, waxes and partial glycerides. In this work we decided to use and to evaluate the following GRAS substances: Precirol™ ATO 5 - glycerylpalmito-stearate, Compritol™ 888 ATO - glyceryldibehenate, Geleol™ Mono and Diglycerides: glycerylmonostearate, Dynasan™ 118 - Tristerin, Softisan™ 100 - hydrogenated coco-glycerides. These ingredients are among the most used to formulate lipid nanoparticles intended for topical application. There are, in fact, thousands of papers in the literature which report the evaluation of lipid nanoparticles prepared by using these substances. The reasons are simple to explain: these excipients are highly biocompatible, endowed with high stability and able to incorporate substances characterized by different chemical features. They are also very cheap and have been used for a long time in the cosmetic field to formulate products which are mostly marketed. The selected excipients are in some cases very different from each other. Glyceryldibehenate, for instance, shows a melting point near 65°C, while hydrogenated coco-glycerides melt near a temperature of 35°C. The differences for example in their melting points, identifies 'low-melting lipids' from 'high-melting lipids' which lead to a different feeling on the skin due to the affinity and different interactions with the lipids of the stratum corneum. Hence the choice was made considering all these aspects. In view of the enhanced pro-oxidant effect of NLC under environmental conditions (Bruge, Damiani et al., 2013), the study was conducted both under standard experimental conditions (no irradiation) and after 10 min UVA-radiation (18

J/cm²) which is approximately equivalent to a dose of UVA radiation achieved after 60 min of sunshine at the French Riviera (Nice) in summer at noon (Seite et al., 1998).

Our data shows that all the tested formulations under standard experimental conditions are well tolerated by dermal fibroblasts and therefore may be considered as biocompatible. In fact, despite a significant decrease in live cells compared to the control in most cases, the percentage of viable cells is always above 80% for all the NLC formulations tested. The mild cytotoxicity may in part be associated with changes in the intracellular ROS content observed. In particular, a highly significant decrease in the percentage of cells showing low intracellular ROS levels was observed in parallel with an increase in cells with an intermediate content of ROS, linking a potential imbalance in oxidative metabolism to the cytotoxicity of nanoparticles. In fact, a pro-oxidant effect of solid-lipid nanoparticles has been reported in the literature although the molecular mechanisms underlying oxidative imbalance have not been investigated in detail (Abbasalipourkabir et al., 2011; Long et al., 2006). Our previous observations pointed out that pro-oxidant and cytotoxic effects of NLC could be further enhanced following exposure to environmental toxic agents (Brüge, Damiani et al., 2013). In fact, when cells were exposed to conditions mimicking environmental ones (i.e. UVA exposure), most of the formulations lead to a significant increase in the percentage of dead cells parallel to an increase in the levels of ROS which is significant for NLC-A and NLC-E. Interestingly, the formulations did not all behave in the same way implying that the lipid composition could be playing a role in modulating these effects. In particular, NLC-C (formulated with Compritol™ 888 ATO) was the only one that resulted totally neutral in terms of cytotoxicity despite a mild pro-oxidant effect which was however, not exacerbated by UVA exposure. This is in accordance with data of Tursilli et al. which showed that solid lipid microparticles based on Compritol 888 ATO significantly enhanced sunscreen photostability (Tursilli et al., 2007), implying that this solid lipid is stable under UV irradiation. On the contrary, NLC-A, NLC-B and NLC-D were influenced by UV exposure since a significant increase in cytotoxicity was observed compared to the irradiated control. In particular, among these, NLC-B showed a significantly higher cytotoxicity even in non-irradiated cells underscoring its lower biocompatibility in general. NLC-B, as reported in Table 1, was formulated using glyceryl monostearate as solid lipid excipient, a well-known ingredient widely used in cosmetic and pharmaceutical fields to produce vehicles intended for topical delivery. Regarding its toxicity on cell viability, there appear to be conflicting results in the literature. Some papers report that glyceryl monostearate is a well-tolerated excipient to formulate both SLN and NLC (Miao et al., 2013; Zhang et al., 2008), while others report that this solid lipid ingredient shows a high cell toxicity (Ying et al., 2011). The cytotoxic effect of glyceryl monostearate seems to be attributed to the presence of stearic acid in its composition (Scholer et al., 2002), although this effect appears to be concentration dependent. Doktorovova and coworkers assessed that concentrations up to 1 mg/mL of stearic acid and its derivatives (glyceryl monostearate) lead to a drastic decrease in cell viability (Doktorovova, Souto et al., 2014). Hence, NLC-B toxicity observed here could depend on the presence of glyceryl monostearate although other factors that could be decisive in the toxicity of these nanoparticles are the amount and surfactant type, the carrier's size and number of dispersed nanoparticles (Mendes et al., 2015). NLC-C was formulated using Compritol 888

360 ATO (glyceryl dibehenate), probably the most popular and widely used solid lipid excipient for both SLN and NLC. There are hundreds of papers in the literature describing the use of this excipient and therefore there is plenty of information regarding its toxicity when used for this purpose. The majority of these papers report no cytotoxicity issues for Compritol 888 ATO, although some authors have stated that SLN formulated using this ingredient showed some toxic effect on cell viability. This was attributed to the longer
365 time needed for degradation of the longer-chain lipids by lipases (Muller et al., 1997). Our results with NLC-C seem to confirm the relative safety on the use of Compritol 888 ATO for formulating lipid nanocarriers.

The application of nanoparticles on the skin is an emerging field for topical delivery of active ingredients into the skin for dermatological and cosmetic applications as well as for transdermal delivery across the skin
370 for systemic treatment. Therefore, having indications on which could be the most suitable candidates for formulating NLC that are biocompatible and non-cytotoxic even when exposed to environmental conditions such as UVA rays present in sunlight that could affect their stability, is of relevance. The results presented here on the comparison of five different, blank, nanostructured lipid carriers may help address this issue and hence direct future choices during the formulation strategies of these delivery systems.

375

ACKNOWLEDGEMENTS

The authors thank the Università Politecnica delle Marche for financial support.

380 REFERENCES

- Abbasalipourkabir, R., Salehzadeh, A., Abdullah, R., 2011. Cytotoxicity effect of solid lipid nanoparticles on human breast cancer cell lines. *Biotechnology* 10, 528-533.
- Bruge, F., Damiani, E., Puglia, C., Offerta, A., Armeni, T., Littarru, G.P., Tiano, L., 2013. Nanostructured lipid carriers loaded with CoQ10: effect on human dermal fibroblasts under normal and UVA-mediated
385 oxidative conditions. *Int J Pharm* 455, 348-56.
- Doktorovova, S., Souto, E.B., Silva, A.M., 2014. Nanotoxicology applied to solid lipid nanoparticles and nanostructured lipid carriers - a systematic review of in vitro data. *Eur J Pharm Biopharm* 87, 1-18.
- Gokce, E.H., Korkmaz, E., Deller, E., Sandri, G., Bonferoni, M.C., Ozer, O., 2012. Resveratrol-loaded solid lipid nanoparticles versus nanostructured lipid carriers: evaluation of antioxidant potential for dermal
390 applications. *Int J Nanomedicine* 7, 1841-50.
- Gonzalez-Mira, E., Egea, M.A., Garcia, M.L., Souto, E.B., 2010. Design and ocular tolerance of flurbiprofen loaded ultrasound-engineered NLC. *Colloids Surf B Biointerfaces* 81, 412-21.
- Hafer, K., Iwamoto, K.S., Schiestl, R.H., 2008. Refinement of the dichlorofluorescein assay for flow cytometric measurement of reactive oxygen species in irradiated and bystander cell populations. *Radiat*
395 *Res* 169, 460-8.

- Huerta-Garcia, E., Perez-Arizti, J.A., Marquez-Ramirez, S.G., Delgado-Buenrostro, N.L., Chirino, Y.I., Iglesias, G.G., Lopez-Marure, R., 2014. Titanium dioxide nanoparticles induce strong oxidative stress and mitochondrial damage in glial cells. *Free Radic Biol Med* 73, 84-94.
- Jaeger, A., Weiss, D.G., Jonas, L., Kriehuber, R., 2012. Oxidative stress-induced cytotoxic and genotoxic effects of nano-sized titanium dioxide particles in human HaCaT keratinocytes. *Toxicology* 296, 27-36.
- Jenning, V., Gohla, S., 2001. Encapsulation of retinoids in solid lipid nanoparticles (SLN). *J Microencapsul* 18, 149-58.
- Joshi, M.D., Muller, R.H., 2009. Lipid nanoparticles for parenteral delivery of actives. *Eur J Pharm Biopharm* 71, 161-72.
- Kuchler, S., Wolf, N.B., Heilmann, S., Weindl, G., Helfmann, J., Yahya, M.M., Stein, C., Schafer-Korting, M., 2010. 3D-wound healing model: influence of morphine and solid lipid nanoparticles. *J Biotechnol* 148, 24-30.
- Kulthong, K., Maniratanachote, R., Kobayashi, Y., Fukami, T., Yokoi, T., 2012. Effects of silver nanoparticles on rat hepatic cytochrome P450 enzyme activity. *Xenobiotica* 42, 854-62.
- Kupetz, E., Bunjes, H., 2014. Lipid nanoparticles: drug localization is substance-specific and achievable load depends on the size and physical state of the particles. *J Control Release* 189, 54-64.
- Long, T.C., Saleh, N., Tilton, R.D., Lowry, G.V., Veronesi, B., 2006. Titanium dioxide (P25) produces reactive oxygen species in immortalized brain microglia (BV2): implications for nanoparticle neurotoxicity. *Environ Sci Technol* 40, 4346-52.
- Mehnert, W., Mader, K., 2001. Solid lipid nanoparticles: production, characterization and applications. *Adv Drug Deliv Rev* 47, 165-96.
- Mendes, L.P., Delgado, J.M., Costa, A.D., Vieira, M.S., Benfica, P.L., Lima, E.M., Valadares, M.C., 2015. Biodegradable nanoparticles designed for drug delivery: The number of nanoparticles impacts on cytotoxicity. *Toxicol In Vitro* doi.org/10.1016/j.tiv.2014.12.021.
- Miao, J., Du, Y.Z., Yuan, H., Zhang, X.G., Hu, F.Q., 2013. Drug resistance reversal activity of anticancer drug loaded solid lipid nanoparticles in multi-drug resistant cancer cells. *Colloids Surf B Biointerfaces* 110, 74-80.
- Muller, R.H., Keck, C.M., 2004. Drug delivery to the brain--realization by novel drug carriers. *J Nanosci Nanotechnol* 4, 471-83.
- Muller, R.H., Mader, K., Gohla, S., 2000. Solid lipid nanoparticles (SLN) for controlled drug delivery - a review of the state of the art. *Eur J Pharm Biopharm* 50, 161-77.
- Muller, R.H., Radtke, M., Wissing, S.A., 2002. Nanostructured lipid matrices for improved microencapsulation of drugs. *Int J Pharm* 242, 121-8.
- Muller, R.H., Ruhl, D., Runge, S., Schulze-Forster, K., Mehnert, W., 1997. Cytotoxicity of solid lipid nanoparticles as a function of the lipid matrix and the surfactant. *Pharm Res* 14, 458-62.
- Muller, R.H., Runge, S., Ravelli, V., Mehnert, W., Thunemann, A.F., Souto, E.B., 2006. Oral bioavailability of cyclosporine: solid lipid nanoparticles (SLN) versus drug nanocrystals. *Int J Pharm* 317, 82-9.

Pardeike, J., Schwabe, K., Muller, R.H., 2010. Influence of nanostructured lipid carriers (NLC) on the physical properties of the Cutanova Nanorepair Q10 cream and the in vivo skin hydration effect. *Int J Pharm* 396, 166-73.

Periasamy, V.S., Athinarayanan, J., Al-Hadi, A.M., Juhaimi, F.A., Alshatwi, A.A., 2014. Effects of titanium dioxide nanoparticles isolated from confectionery products on the metabolic stress pathway in human lung fibroblast cells. *Arch Environ Contam Toxicol* 68, 521-33.

Puglia, C., Bonina, F., 2012. Lipid nanoparticles as novel delivery systems for cosmetics and dermal pharmaceuticals. *Expert Opin Drug Deliv* 9, 429-41.

Puglia, C., Bonina, F., Rizza, L., Blasi, P., Schoubben, A., Perrotta, R., Tarico, M.S., Damiani, E., 2012. Lipid nanoparticles as carrier for octyl-methoxycinnamate: in vitro percutaneous absorption and photostability studies. *J Pharm Sci* 101, 301-11.

Scholer, N., Hahn, H., Muller, R.H., Liesenfeld, O., 2002. Effect of lipid matrix and size of solid lipid nanoparticles (SLN) on the viability and cytokine production of macrophages. *Int J Pharm* 231, 167-76.

Seite, S., Moyal, D., Richard, S., de Rigal, J., Leveque, J.L., Hourseau, C., Fourtanier, A., 1998. Mexoryl SX: a broad absorption UVA filter protects human skin from the effects of repeated suberythemal doses of UVA. *J Photochem Photobiol B* 44, 69-76.

Teeranachaideekul, V., Souto, E.B., Junyaprasert, V.B., Muller, R.H., 2007. Cetyl palmitate-based NLC for topical delivery of Coenzyme Q(10) - development, physicochemical characterization and in vitro release studies. *Eur J Pharm Biopharm* 67, 141-8.

Tursilli, R., Piel, G., Delattre, L., Scalia, S., 2007. Solid lipid microparticles containing the sunscreen agent, octyl-dimethylaminobenzoate: effect of the vehicle. *Eur J Pharm Biopharm* 66, 483-7.

Venditti, E., Spadoni, T., Tiano, L., Astolfi, P., Greci, L., Littarru, G.P., Damiani, E., 2008. In vitro photostability and photoprotection studies of a novel 'multi-active' UV-absorber. *Free Radic Biol Med* 45, 345-54.

Xia, T., Kovochich, M., Brant, J., Hotze, M., Sempf, J., Oberley, T., Sioutas, C., Yeh, J.I., Wiesner, M.R., Nel, A.E., 2006. Comparison of the abilities of ambient and manufactured nanoparticles to induce cellular toxicity according to an oxidative stress paradigm. *Nano Lett* 6, 1794-807.

Ying, X.-Y., Cui, D., Yu, L., Du, Y.-Z., 2011. Solid lipid nanoparticles modified with chitosan oligosaccharides for the controlled release of doxorubicin. *Carbohydr Polym* 84, 1357-1364.

Yue, Y., Zhou, H., Liu, G., Li, Y., Yan, Z., Duan, M., 2010. The advantages of a novel CoQ10 delivery system in skin photo-protection. *Int J Pharm* 392, 57-63.

Zhang, X.G., Miao, J., Dai, Y.Q., Du, Y.Z., Yuan, H., Hu, F.Q., 2008. Reversal activity of nanostructured lipid carriers loading cytotoxic drug in multi-drug resistant cancer cells. *Int J Pharm* 361, 239-44.

470 **Figure legends**

Fig. 1 - Percentage of viable, apoptotic and dead cells in HDF treated for 24 h with the five different NLC formulations (A-E), non-irradiated (panel A) or irradiated with UVA (18 J/cm²) (panel B). Analyses were conducted after exposure to the NLC formulations, and after UVA irradiation. Data are expressed as mean ± S.D. *p < 0.05 vs CTRL.

475

Fig. 2 - Intracellular levels of ROS in HDF treated for 24 h with the five different NLC formulations (A-E), non-irradiated (panel A) or irradiated with UVA (18 J/cm²) (panel B). Percentage of cells presenting low (□), mid (■) and high (■) intracellular levels of ROS are expressed in terms of carboxy-H₂DCFDA fluorescence. Data are expressed as mean ± S.D. *p < 0.05 vs CTRL.

480

485

490

495

500

Figure 1

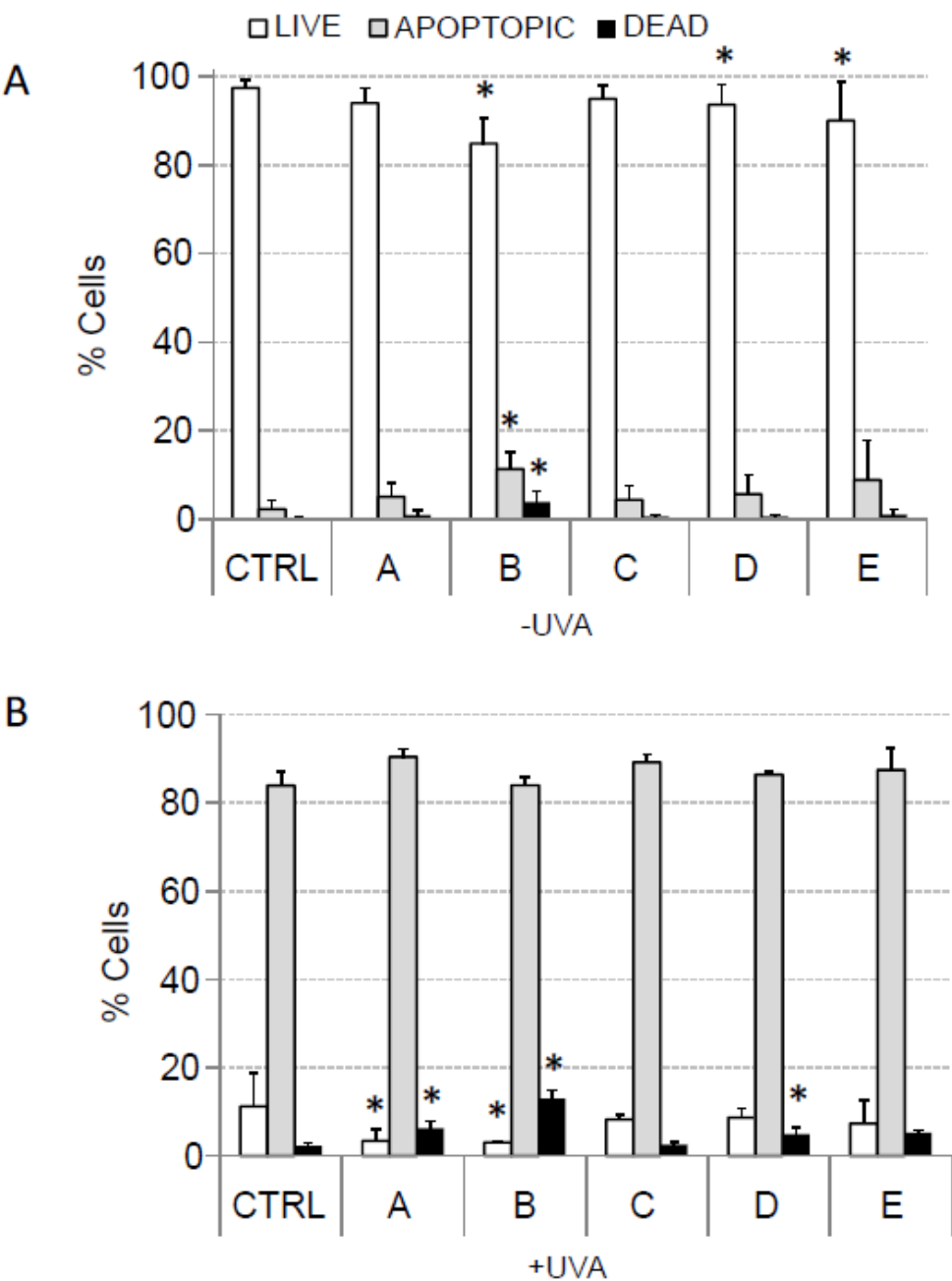


Figure 2

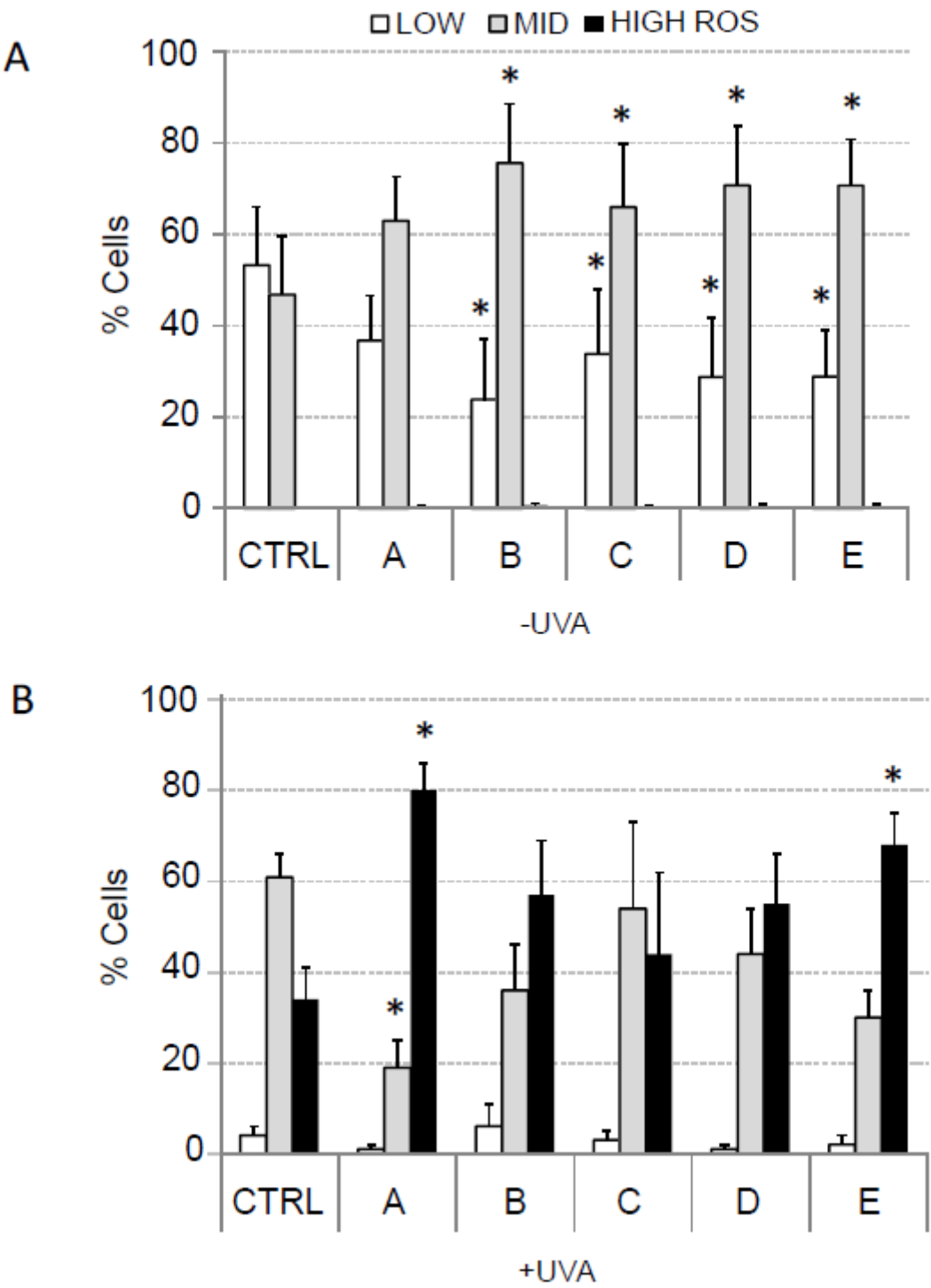


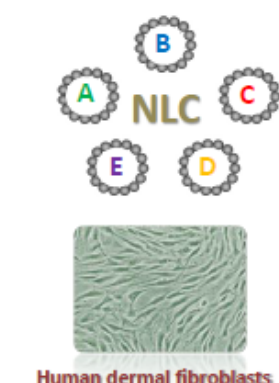
Table 1. Composition (%) of the NLC suspensions A-E

Ingredients	Formulations				
	A	B	C	D	E
Compritol™ 888 ATO	-----	-----	1.15	-----	-----
Dynasan™ 118	1.15	-----	-----	-----	-----
Geleol™ Mono Diglyc.	-----	1.15	-----	-----	-----
Precirol™ ATO 5	-----	-----	-----	1.15	-----
Softisan™ 100	-----	-----	-----	-----	1.15
Miglyol™ 812	0.5	0.5	0.5	0.5	0.5
Lutrol™ F68	0.05	0.05	0.05	0.05	0.05
Distilled water	98.3	98.3	98.3	98.3	98.3

Table 2. Particle size, polydispersity index (PDI) and zeta potential of the studied NLC formulations.

	A	B	C	D	E
<i>Particle size (nm)</i>	56.8 ± 8.3	55.4 ± 7.2	69.0 ± 8.7	42.9 ± 5.9	122.1 ± 10.9
<i>Polydispersity index</i>	0.25 ± 0.1	0.3 ± 0.08	0.26 ± 0.09	0.18 ± 0.04	0.44 ± 0.07
<i>Zeta Potential (mV)</i>	-29.4 ± 1.3	-36.3 ± 1.8	-32.1 ± 1.5	-40.5 ± 2.6	-33.3 ± 2.1

Graphical Abstract



Ingredients	Formulations (%)				
	A	B	C	D	E
Compritol™ 888 ATO	----	----	1.15	----	----
Dynasan™ 118	1.15	----	----	----	----
Geleol™ Mono Diglyc.	----	1.15	----	----	----
Precirol™ ATO 5	----	----	----	1.15	----
Softisan™ 100	----	----	----	----	1.15
Miglyol™ 812	0.5	0.5	0.5	0.5	0.5
Lutrol™ F68	0.05	0.05	0.05	0.05	0.05
Distilled water	98.3	98.3	98.3	98.3	98.3

